Int J Appl Earth Obs Geoinformation 72 (2018) 76–85

Contents lists available at ScienceDirect

Int J Appl Earth Obs Geoinformation

journal homepage: www.elsevier.com/locate/jag

Surface soil moisture retrievals over partially vegetated areas from the synergy of Sentinel-1 and Landsat 8 data using a modified water-cloud model

Yansong Bao[a,b,*], Libin Lin[a,b], Shanyu Wu[a,b], Khidir Abdalla Kwal Deng[a,b], George P. Petropoulos[c,d,e]

[a] Collaborative Innovation Center on Forecast and Evaluation of Meteorological Disasters, Key Laboratory for Aerosol-Cloud-Precipitation of China Meteorological Administration, Nanjing University of Information Science & Technology, Nanjing 210044, China
[b] School of Atmospheric physics, Nanjing University of Information Science and Technology, Nanjing 210044, China
[c] Department of Soil Water Resources, Institute of Industrial & Forage Crops, Hellenic Agricultural Organization "Demeter", Larisa, Greece
[d] Department of Geography and Earth Sciences, University of Aberystwyth, SY23 3DB, Wales, UK
[e] Department of Mineral Resources Engineering, Technical University of Crete, 73100, Chania, Crete, Greece

ARTICLE INFO

Keywords:
Surface soil moisture
Vegetation water content
Water-cloud model
Sentinel-1 SAR
Landsat 8 OLI

ABSTRACT

In this study, is presented a new methodology for retrieving surface soil moisture (SSM) under conditions of partial vegetation cover based on the synergy between Sentinel-1 Synthetic Aperture Radar (SAR) and Landsat Operational Land Image (OLI) data. To remove the effect of vegetation on SSM retrieval, the Landsat OLI spectral index is applied to build a model for the vegetation water content estimation. The model is substituted into the original water-cloud model, and thus a modified water-cloud model with a spectral index is built. Additionally, an SSM estimation model is developed based on the modified water-cloud model. The technique was tested at two experimental sites in the UK and Spain on which reference data of SSM are acquired operationally by ground observational networks. In overall, the key findings of our study were: (1) For a vegetation-covered surface, the normalized difference water index (NDWI) obtained from the 1.57–1.65 μm band reflectance data was the most suitable for removing the effects of vegetation cover on soil water content estimation; (2) Compared to the Sentinel-1 VH polarization, the backscattering coefficient at VV polarization was more suitable for soil moisture retrieval and obtained a higher accuracy; (3) The developed model could be used to retrieve SSM under vegetation cover with a high accuracy that indicates the correlation coefficient (R) between the estimated and measured soil moisture was 0.911 and that the root mean square error (RMSE) was 0.053 cm3/cm3; (4) The model can be used to retrieve regional SSM with a high spatial and temporal resolution. Our methodology for deriving SSM offers a number of advantages for many practical applications and research alike and its use by the wider community remains to be seen.

1. Introduction

Surface soil moisture (SSM), defined as the content of water contained in the first 0–5 cm of the soil layer, is an important parameter in the field of atmospheric science and agricultural science (Hégaratmascle et al., 2002; Anagnostopoulos et al., 2017; Petropoulos et al., 2018). In the field of atmospheric science, soil moisture is an important variable in the study of seasonal climate evolution and prediction, playing a key role in the quality and energy conversion between the soil and atmosphere (Seneviratne et al., 2010; Torres-Rua et al., 2016). In agricultural sciences, soil moisture is a key indicator for crop yield estimation, drought monitoring and prediction (Bolten et al., 2010; Pablos et al., 2017; Whyte et al., 2018). At a regional scale, soil moisture information is important for local agriculture and water management. Moreover, at a global scale, soil moisture is of great value for weather forecasting, climate change and monitoring floods (Leroux et al., 2007; Piles et al., 2016). Soil moisture information is also indispensable in the study of the land surface process and numerical weather prediction, and it plays an important role in improving the prediction results of regional and global climate models (Mao et al., 2008). However, due to its large spatial heterogeneity and the high cost of soil moisture observation equipment, it is very difficult to establish

* Corresponding author at: Collaborative Innovation Center on Forecast and Evaluation of Meteorological Disasters, Key Laboratory for Aerosol-Cloud-Precipitation of China Meteorological Administration, Nanjing University of Information Science & Technology, Nanjing 210044, China.
E-mail address: ysbao@nuist.edu.cn (Y. Bao).

https://doi.org/10.1016/j.jag.2018.05.026
Received 30 March 2018; Accepted 30 May 2018

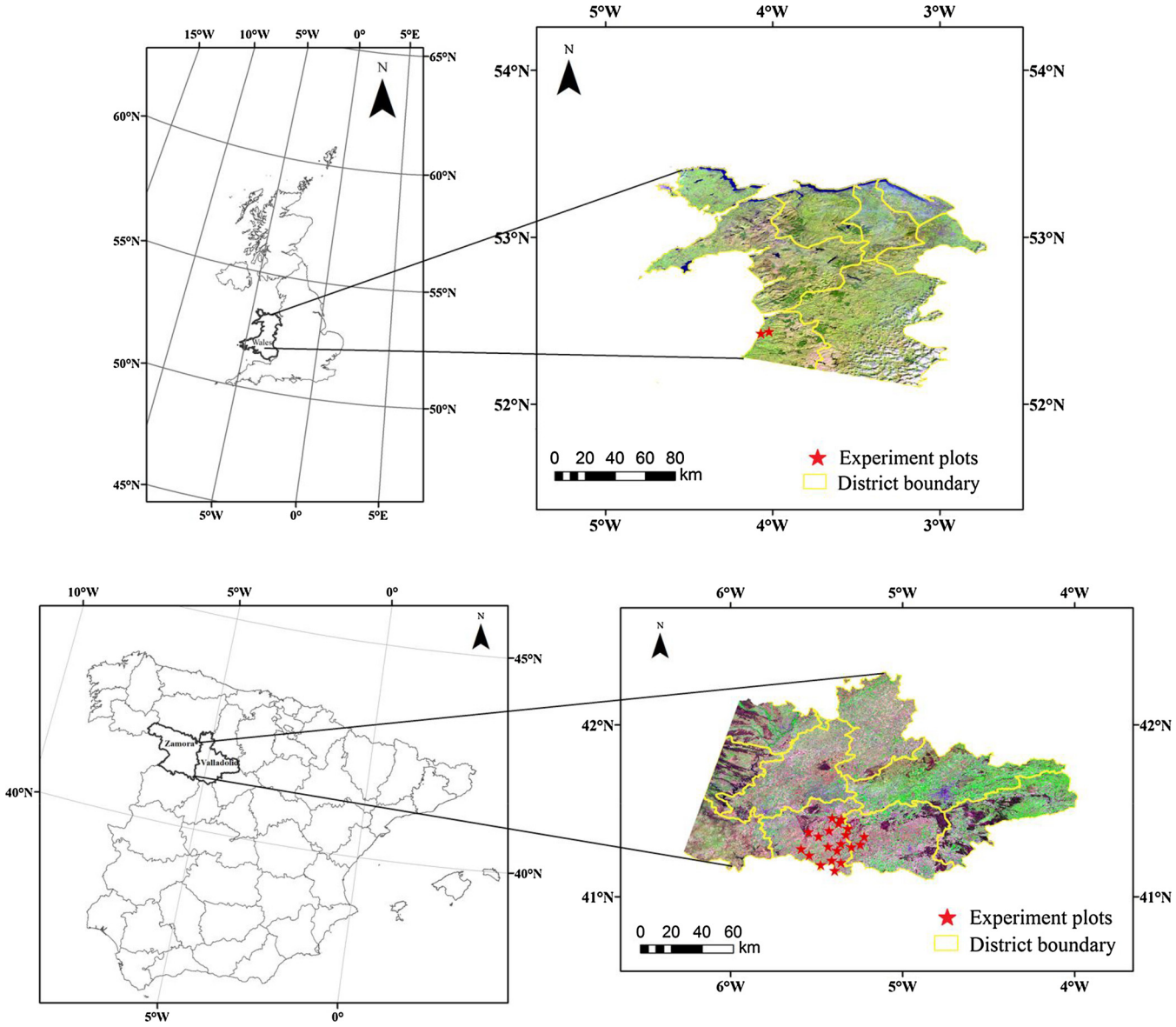

Fig. 1. Distribution of sampling points in the UK (top) and Spain (bottom).

high-resolution observation networks at regional and global scales (Lu et al., 2014).

Retrieving soil moisture with Earth Observation (EO) technology has been explored for more than, 30 years. The main methods employed are retrieving soil moisture from spectral information acquired in the optical, thermal infrared and microwave (MW) domains of the electromagnetic spectrum (Bao et al., 2014; Baghdadi et al., 2016; Zhang and Zhou, 2016; Santamaria-Artigas et al., 2016). In the optical methods, soil moisture is estimated via the computation of spectral reflectance indices, linking the changes in the spectral characteristics with the soil moisture content. Those methods are straightforward to be implemented but can be easily affected by weather conditions. Most of the thermal infrared methods estimate soil moisture through the soil thermal characteristics, via the computation of parameters such as the thermal inertia (Verstraeten et al., 2006). However, in an area with high vegetation coverage, the soil radiation information is concealed by the vegetation canopy, which will affect the accuracy of the soil moisture estimation. Therefore, those methods are generally applicable only for monitoring soil moisture in bare soil and sparsely vegetated areas and under cloud-free conditions. However, microwave radiation at longer wavelengths has a stronger penetrating ability, which is not affected by weather conditions and/or acquisition time. Therefore, MW remote sensing, or the synergy of MW with information acquired in other regions of the electromagnetic radiation spectrum, is considered as one of the most promising avenues for SSM monitoring (Tian, 1991; Petropoulos et al., 2014).

A new generation of Sentinel-1 satellites launched by the European Space Agency (ESA), which operate in constellation, began to provide near-real-time synthetic aperture radar data (SAR). These were the first satellites to provide free near-real-time high spatial (5 m × 5 m) and high temporal resolution (6 days) data. Based on the simulated Sentinel-1 SAR data, Paloscia et al. developed an approach based on the Artificial Neural Network (ANN) algorithm to conduct soil moisture retrieval in Italy, Australia and Spain, and the results showed that such high spatio-temporal resolution as that from Sentinel-1 data make soil moisture real-time monitoring possible (Paloscia et al., 2013). He et al. used multi-temporal Sentinel-1 SAR data to estimate SSM over agricultural fields based on the alpha approximation approach (He et al., 2016). The root mean square error (RMSE) of the estimated SSM was 0.06 cm^3/cm^3. Based on the latest Sentinel-1 data and the characteristics of the surface parameters of the experiment area, Wang et al. developed a soil moisture model over the oasis region using the AIEM

model (Wang et al., 2017). However, the correlation coefficient between the measured and estimated soil moisture was only 0.76. Zeng et al. studied the effect of different polarization combinations on soil moisture estimation in different vegetation covers based on Sentinel-1 A data using the support vector regression algorithm, and concluded that only combined VV polarization with normalized difference vegetation index (NDVI) can get high retrieval accuracy. However, the overall effect was not ideal (Zeng et al., 2017). Based on multi-temporal Sentinel-1 and Landsat 8 satellite images, Alexakis et al. used ANN algorithm to estimate the top soil Soil Moisture Content, and coefficient of determination (R^2) values was between 0.7 and 0.9 (Alexakis et al., 2017). The above studies are some of those already published advocating the promise and suitability of Sentinel-1 for the SSM retrievals over partially vegetated areas. Yet, in most of the published studies, accuracy in SSM retrievals has been reported low, especially over partially vegetated areas, indicating the necessity of further work to be conducted in this direction.

In purview of the above, the present study aims at developing a technique that allows the combined use of Sentinel-1 SAR and Landsat OLI data for SSM retrievals over partially vegetated areas. In order to remove vegetation water content effects on SSM estimation, the Landsat OLI spectral index is applied to establish an inversion model for the vegetation water content estimation. The model is combined with the original water-cloud model, and a modified water-cloud model with a spectral index was built. Additionally, a soil moisture retrieval model is developed based on the modified water-cloud model over vegetated areas. The ability of our proposed method to provide spatiotemporal estimates of SSM is also demonstrated herein using reference data from the selected *in-situ* monitoring networks based in the UK and Spain.

2. Datasets and pre-processing

2.1. Study sites and ground measurements

To develop the soil water content estimation model under vegetation cover conditions, 2 study areas were selected with variant vegetation cover and terrain properties located in Wales and in Spain belonging to the Wales Soil Moisture Network (WSMN) (Petropoulos and McCalmont, 2017) (Fig. 1) and REMEDHUS Network (González-Zamora et al., 2015) (Fig. 2) respectively. The two study areas are dominated by plains, and the main surface types are agricultural land, natural vegetation, sparse vegetation (herbaceous plants), grassland, urban and construction areas, permanent wetlands and water. Both sites are part of *in-situ* monitoring networks and the data measured from each site are distributed for free from the International Soil Moisture Network (ISMN) (Dorigo et al., 2011). The ISMN was co-established by the Global Energy and Water Exchanges Project (GEWEX), the Group of Earth Observation (GEO) and the Committee on Earth Observation Satellites (CEOS), and the observatory can provide global site soil moisture data.

The soil volumetric moisture at the 0 to 5 cm depth was obtained from the *in-situ* monitoring networks. For the UK, soil volumetric moisture data at four sites were acquired from January 1, 2015 to December 31, 2016. For the Spanish sites, the SSM at 20 sites were obtained covering the period from January 1, 2015 to December 31, 2015. The main information of the experimental sites is summarized in Table 1.

2.2. Landsat 8 data acquisition and processing

To eliminate the effect of vegetation on the soil moisture estimation, the Landsat 8 OLI data were used in this study. The OLI instrument includes nine shortwave spectral bands, and the data used in this study have the resolution of 30 m. The Landsat 8 images are provided at no cost for global users through the data distribution website (https://glovis.usgs.gov/) of the United States Geological Survey (USGS). To avoid the effect of cloud contamination on data analysis, non-cloud or less-cloud images were acquired. For the UK areas, eight images from 22 March, 7 April, 23 April, and 10 June 2015 as well as 20 January, 15 August, 31 August, and 2 October 2016 were acquired. For the Spain areas, five images from 19 January, 8 March, 27 May, 14 July, and 30 July 2015 were acquired (Table 3). For the original images, a radiometric calibration was conducted, and the calibration equation is as follows:

$$L_\lambda = M_L Q_{cal} + A_L \quad (1)$$

Where L_λ is the radiation at the top of the atmosphere, M_L is the band-specific multiplicative rescaling factor from the metadata, Q_{cal} is the quantitative and calibrated standard product digital number value, and A_L is the band-specific additive rescaling factor from the metadata.

To reduce the atmosphere effect and obtain the reflectance data, the atmosphere correction was conducted with the Fast Line-of-sight Atmosphere Analysis of Spectral Hypercube (FLAASH) tool. Then, the reflectance images were geometrically corrected, and a series of vegetation indices, such as Normalized Difference Vegetation Index (NDVI) (Rouse et al., 1973), Enhanced Vegetation Index (EVI) (Huete et al., 1994) and Normalized difference water index (NDWI) (Gao, 1996), were calculated. In addition, the supervised classification method was used to retrieve crop field cover under clear–sky conditions from OLI images. The experiments in this study were conducted in the crop fields under clear-sky condition.

2.3. Sentinel-1 SAR data acquisition and processing

In order to develop a methodology for SSM retrieval from SAR satellite images, we obtained thirteen images of Sentinel-1 SAR data in this study. Sentinel-1 satellites are an important part of Global Monitoring for Environment and Security (GMES), co-sponsored by the European Commission and the European Space Agency. Sentinel-1 contains two satellites: the first satellite (Sentinel-1A) was launched on 3 April 2014, and the second satellite (Sentinel-1B) was launched on 25 April 2016. According to the data acquisition mode of the satellites, 5 ~ 40 m resolution images can be obtained in all-weather conditions. The revisit cycle of one satellite was 12 days, which decreased to 6 days using two satellites. Sentinel-1 equipped with a C-band SAR sensor with an operating frequency of 5.4 GHz has a multi-polarization imaging capability. The Sentinel-1 imaging system has four imaging modes: stripmap model (SM), interferometric wide swath (IW), extra-wide swath (EW), and wave mode (WM), shown in Table 2. The data used in this study were the S1 TOPS-mode SLC data from an interferometric wide (IW) swath mode. The imaging model solves the scalloping effect of wide synthetic aperture radar imaging and enhances the imaging radiation performance, which provides more accurate extracted backscattering coefficients (Zeng et al., 2017).

In the UK areas, eight Sentinel-1 images from 24 March, 5 April, 22 April, and 9 June 2015 as well as 20 January, 14 August, 30 August, and 2 October 2016 were acquired to ensure consistency in the acquisition time between the Sentinel-1 SAR and Landsat-8 OLI data. Similarly, in the Spain areas, five Sentinel-1 images from 20 January, 9 March, 26 May, 13 July and 31 July 2015 were acquired (Table 3). The acquired SAR images are level-1B data, which need to be pre-processed before being analyzed. To effectively eliminate the speckle noise while preserving the edge information of the image, the Refined Lee filter method was used (He et al., 2016; Lee et al., 1994). In addition, the SARscape 5.2.1 tool was used to conduct the geocoding and radiometric calibration to obtain the backscattering coefficient data of the experiment area. The radiometric calibration was conducted based on the following expression:

$$\sigma_{ij}^0 = 10\, log_{10}\left(\frac{DN_{i,j}^2}{A_\sigma^2}\right) \quad (2)$$

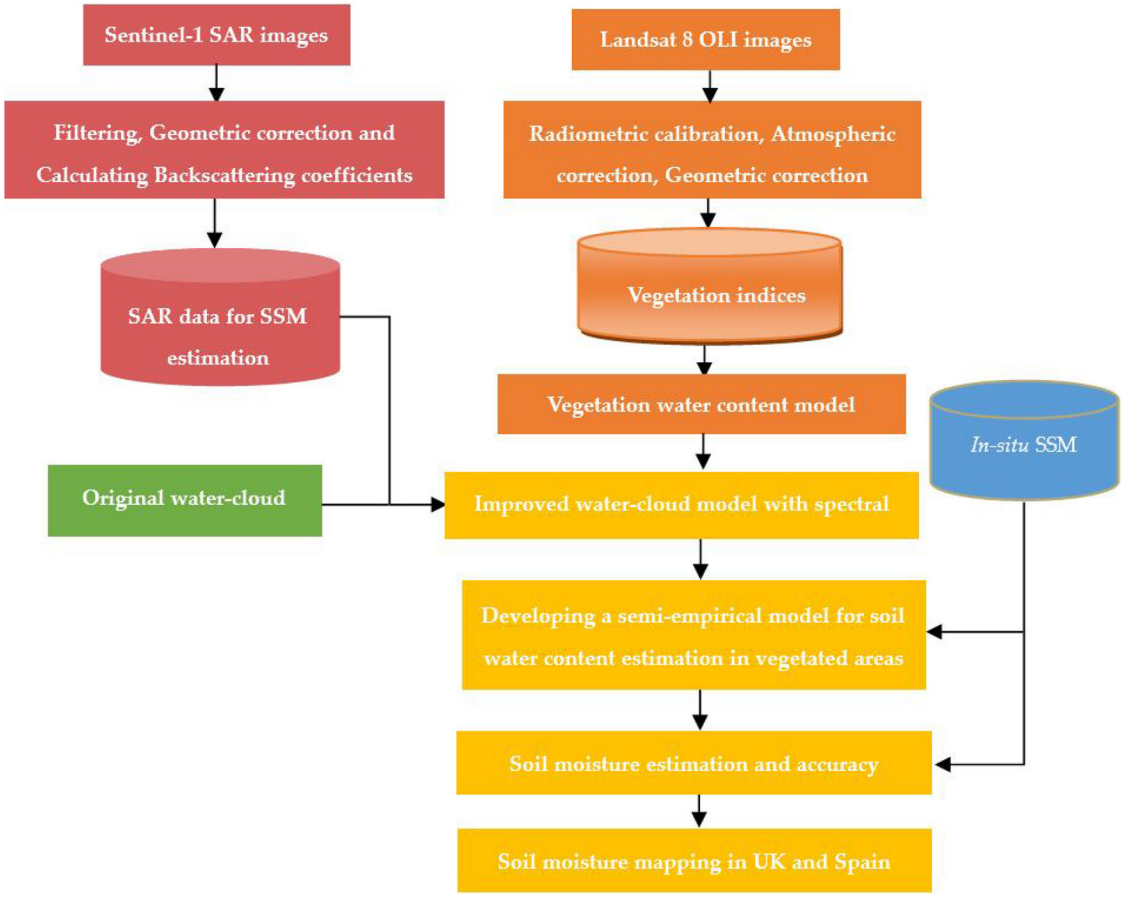

Fig. 2. Flowchart for estimating the soil water content in vegetation-covered areas based on Sentinel-1 SAR and Landsat 8 OLI data.

Where σ^0 is the backscattering coefficient (dB); i and j represent the i-th row and the j-th column, respectively; $DN_{i,j}$ is the digital number of the SAR image; and A_σ is the calibration parameter.

3. Methodology

A procedure of developing the methodology for SSM estimation is illustrated in Fig. 2. First, in order to obtain SAR data for SSM estimation, the acquired Sentinel-1 SAR images were processed, and the

Table 1
Summary of the main characteristics of the soil moisture in-situ monitoring sites used in this study.

Country	Station	Longitude	Latitude	Altitude(m)	Vegetation cover type
UK	Commins Coch	4.020556W	52.432222N	30	Agriculture / grassland
	Commins Coch	4.021389W	52.432222N	31	
	Penglais	4.068333 W	52.422222N	114	Miscanthus
	Penglais	4.070556 W	52.421389N	110	
Spain	Canizal	5.35861 W	41.1972N	720	Herbaceous
	Carretoro	5.37972 W	41.26611N	745	Herbaceous
	Casa_Periles	5.3201 W	41.39508N	750	Herbaceous
	Concejo_del_Monte	5.24569 W	41.30126N	765	Herbaceous
	El_Coto	5.42786 W	41.38251N	720	Herbaceous
	El_Tomillar	5.48891 W	41.35004N	755	Herbaceous
	Granja_g	5.35925 W	41.3069N	720	Herbaceous
	Guarrati	5.43402 W	41.2905N	720	Herbaceous
	La_Atalaya	5.39621 W	41.15011N	830	Herbaceous
	La_Cruz_de_Elias	5.29868 W	41.28662N	795	Herbaceous
	Las_Arenas	5.54714 W	41.37455N	745	Herbaceous
	Las_Bodegas	5.47572 W	41.18381N	900	Herbaceous
	Las_Brozas	5.35734 W	41.44765N	675	Herbaceous
	Las_Eritas	5.41224 W	41.20843N	835	Herbaceous
	Las_Tres_Rayas	5.59056 W	41.27611N	870	Herbaceous
	Las_Vacas	5.22361 W	41.34778N	770	Herbaceous
	Las_Victorias	5.37267 W	41.42529N	740	Herbaceous
	Llanos_de_la_Boveda	5.32977 W	41.35873N	790	Herbaceous
	Paredinas	5.40964W	41.45703N	665	Herbaceous
	Zamarron	5.54291 W	41.2404N	885	Herbaceous

Table 2
Characteristics of the various imaging modes of Sentinel-1 SAR.

Model	Incident angle /°	Resolution	Width /km
SM	20 ~ 45	5 m × 5 m	80
IW	29 ~ 45	5 m × 20 m	250
EW	19 ~ 47	20 m × 40 m	400
MW	22 ~ 38	5 m × 5 m	20 × 20

backscattering coefficient images in experiment areas were obtained. Then, the backscattering coefficients of each sample were extracted according to the latitude and longitude coordinates. In addition, the acquired Landsat 8 OLI images were processed, and the vegetation index images covering the geographical extend of the experimental areas were obtained. Then, the vegetation indices of each sample were extracted according to the latitude and longitude coordinates.

To develop a semi-empirical model for the soil water content estimation, the water-cloud model was used. There are two important parameters in the water-cloud model. One is the vegetation water content, which can be expressed by vegetation indices obtained from Landsat 8 data. Another one is the soil backscattering coefficient, which can be simply described by using a linear correlation with SSM. Then, those expressions were substituted into the water-cloud model, and an improved water-cloud model with a spectral index was built. In addition, a semi-empirical model for SSM estimation was built.

In this study, we obtained 8 satellite images in UK and 5 images in Spain. Combined with *in-situ* measurement of the International Soil Moisture Observation Network, 102 samples were obtained. These data were grouped randomly. One group (51 samples) was used to fit the coefficients of the semi-empirical model by a best-fitting method, and another group (51 samples) was used to validate the model. The correlation coefficient and root mean square error of the estimated SSM were calculated to evaluate the accuracy of the soil moisture estimation model. Finally, in order to verify the applicability of the semi-empirical model, the model was used to map the soil moisture in the UK and Spain.

3.1. Water-cloud model

The canopy backscattering model is an important tool for studying the relationship between ground backscattering and soil moisture. To better describe the backscattering of the soil and vegetation in vegetation-covered areas, the water-cloud model proposed by Attema and Ulaby in 1978 was used in this study. The water-cloud model is based on the radiation transport model, and the vegetation canopy is assumed to be uniform horizontal clouds, thus ignoring multiple scattering. In the water-cloud model, the total backscattering in the vegetation-covered areas can be simply described as two parts: one is the scattering reflected directly from the vegetation canopy, and the second is the backscattering from the ground (Kumar et al., 2015). The model is relatively simple and practical in describing radar scattering mechanisms in crop-covered areas. Therefore, this model has often been used to estimate relevant information in vegetation-covered areas (Pierdicca et al., 2013).For example, Attema & Ulaby used it to estimate soil moisture in crop-covered areas (Attema and Ulaby, 1978).

The water-cloud model is expressed as:

$$\sigma^0 = \sigma^0_{veg} + T^2\sigma^0_{soil} \tag{3}$$

$$\sigma^0_{veg} = AM_v\cos(\theta)(1-T^2) \tag{4}$$

$$T^2 = \exp(-2BM_v\sec(\theta)) \tag{5}$$

Where σ^0 is the total canopy backscattering coefficient (dB); σ^0_{veg} is the vegetation backscattering coefficient; σ^0_{soil} is the soil backscattering coefficient (dB). M_v is the vegetation water content (kg/m^2); T^2 is a double attenuation factor for radar waves passing through vegetation; θ is incident angle (°).

3.2. Vegetation water content estimation from the optical remote sensed data

In the water-cloud model, the vegetation water content is one of the most important parameters. In order to remove the influence of the vegetation canopy on soil moisture estimation, the vegetation water content needs to be acquired. Published studies indicated that the vegetation indices obtained from satellite data could be used for the vegetation water content estimation (Zhang et al., 2010). The vegetation indices commonly used for vegetation water content estimation includes NDVI (Prakash et al., 2012), EVI (Bai et al., 2016) and NDWI (Zheng et al., 2014). These vegetation indices were calculated as follows:

$$NDVI = \frac{R_{NIR}-R_{RED}}{R_{NIR}+R_{RED}} \tag{6}$$

$$EVI = 2.5\times\frac{R_{NIR}-R_{RED}}{R_{NIR}+6.0R_{RED}-7.5R_{BLUE}+1} \tag{7}$$

$$NDWI = \frac{R_{NIR}-R_{SWIR}}{R_{NIR}+R_{SWIR}} \tag{8}$$

Where R_{NIR} is the reflectivity at the near infrared band; R_{RED} is the reflectivity at the red band; R_{BLUE} is the reflectivity at the blue band; R_{SWIR} is the reflectivity at the shortwave infrared band. In this study, the vegetation indices obtained from Landsat 8 OLI data were used to estimate the vegetation water content in the study areas. Since the Landsat 8 data has two shortwave infrared bands: SWIR1 (band range: 1.57–1.65 μm) and SWIR2 (band range: 2.11–2.29 μm). In this study, the two shortwave infrared bands were used to establish the NDWI index: NDWI1 and NDWI2, testing their effect on soil moisture

Table 3
List of satellite and ground data acquired over study area.

country	data type	Time of acquisition	data type	Time of acquisition	data type	Time of acquisition
UK	Sentinel-1	24 March 2015	Landsat 8	22 March 2015	*In-situ*	24 March 2015
	Sentinel-1	5 April 2015	Landsat 8	7 April 2015	*In-situ*	5 April 2015
	Sentinel-1	22 April 2015	Landsat 8	23 April 2015	*In-situ*	22 April 2015
	Sentinel-1	9 June 2015	Landsat 8	10 June 2015	*In-situ*	9 June 2015
	Sentinel-1	20 January 2016	Landsat 8	20 January 2016	*In-situ*	20 January 2016
	Sentinel-1	14 August 2016	Landsat 8	15 August 2016	*In-situ*	14 August 2016
	Sentinel-1	30 August 2016	Landsat 8	31 August 2016	*In-situ*	30 August 2016
	Sentinel-1	2 October 2016	Landsat 8	2 October 2016	*In-situ*	2 October 2016
Spain	Sentinel-1	20 January 2015	Landsat 8	19 January 2015	*In-situ*	20 January 2015
	Sentinel-1	9 March 2015	Landsat 8	8 March 2015	*In-situ*	9 March 2015
	Sentinel-1	26 May 2015	Landsat 8	27 May 2015	*In-situ*	26 May 2015
	Sentinel-1	13 July 2015	Landsat 8	14 July 2015	*In-situ*	13 July 2015
	Sentinel-1	31 July 2015	Landsat 8	30 July 2015	*In-situ*	31 July 2015

retrieval.

Previous studies have shown that the relationships between the vegetation water content and vegetation indices are linear (Jackson et al., 2004; Chen et al., 2005; Huang et al., 2009), one-variable quadratic (Maggioni et al., 2006; Yi et al., 2007; Jiang et al., 2015) or exponential (Zheng et al., 2014; Cheng et al., 2014). Considering the accuracy of the vegetation water content estimation and the simplicity of the equation, in this study, one-variable quadratic model was used to estimate the vegetation water content:

$$M_V = aVI^2 + bVI + C \quad (9)$$

3.3. Building a soil water content estimation model

Previous studies have shown that there is a good linear correlation between the soil backscattering coefficient and SSM (Zribi and Dechambre, 2003; Mattia et al., 2006). Therefore, the soil backscattering coefficient σ^0_{soil} can be described by soil volumetric moisture SSM:

$$\sigma^0_{soil} = cSSM + d \quad (10)$$

In order to build SSM estimation model, Eqs. (9) and (10) were substituted into the water-cloud model. In addition, the term $\exp(-2BM_v\sec(\theta))$ was expanded with the Taylor approximation. Finally, a semi-empirical model for the soil water content estimation was developed:

$$SSM = k_1 + k_2\sigma^0 + k_3VI + k_4VI^2 + k_5VI^3 + k_6VI^4 + k_7\sigma^0 sec\theta + k_8\sigma^0 VIsec\theta + k_9\sigma^0 VI^2 sec\theta \quad (11)$$

Where SSM is soil volumetric moisture (cm^3/cm^3); σ^0 is the VH or VV backscattering coefficients (dB) obtained from Sentinel-1 SAR data, VI is the spectral index obtained from Landsat 8 OLI data. θ is the SAR incidence angle(°); $k_1 \sim k_9$ could be obtained by a best-fitting regression method.

4. Results and discussion

4.1. Soil water content estimation from Sentinel-1 SAR data

The developed SSM estimation models were used to retrieve soil moisture from Sentinel-1 SAR data combining the Landsat vegetation indices. The agreement between the modeled SSM and the measured soil volumetric moisture was evaluated on the basis of statistical metrics, namely the correlation coefficient (R) and the root mean square error (Table 4). Table 4 shows the R and RMSE between the estimated and measured SSM based on the 102 sample data.

Comparing the inversion results from Sentinel-1 VH and VV polarization data, the accuracy of the soil moisture estimation from the VV polarization data was significantly higher than that from the VH polarization data. For example, combining NDWI1, the experiments with VV polarization data obtained higher SSM accuracy compared to with VH data (VH: R = 0.807, RMSE = 0.074 cm^3/cm^3; VV: R = 0.911, RMSE = 0.053 cm^3/cm^3). A possible reason for this result is that the VV backscattering coefficient is generally more sensitive to the change in soil water content compared to VH polarization (Patel et al., 2006; Chauhan and Srivastava, 2016).

Table 4
Correlation and root mean square errors between measured and estimated soil volumetric moisture values based on the 102 sample data.

R and RMSE	NDVI	EVI	NDWI1	NDWI2
VH	R = 0.699 RMSE = 0.089	R = 0.754 RMSE = 0.082	R = 0.807 RMSE = 0.074	R = 0.81 RMSE = 0.074
VV	R = 0.755 RMSE = 0.085	R = 0.853 RMSE = 0.065	R = 0.911 RMSE = 0.053	R = 0.894 RMSE = 0.0595

Comparing the performances of the various vegetation indices in SSM estimation, NDWI obtained the better result. This observation can be explained by the fact that generally the SWIR channel is more sensitive to the vegetation water content (Ceccato et al., 2002a, b). Comparing NDWI1 with SWIR1 (1.57–1.65 μm) and NDWI2 with SWIR2 (2.11–2.29 μm),the SSM estimation model with NDWI1 obtained a higher accuracy, which is because the SWIR1 band data have a higher correlation with vegetation water content (ELVIDGE and LYON, 1985). As the SWIR1 band data can acquire more accurate vegetation water content (Chuvieco et al., 2002), they can more effectively remove the effect of vegetation on SSM estimation.

Based on the previous conclusion, the Sentinel-1 VV polarization data and normalized difference water index obtained from Landsat 8 1.57–1.65 μm band were selected to study the methodology for SSM estimation. The coefficients $k_1 \sim k_9$ in Eq. (11) were obtained by using the best-fitting method based on the 51 training sample data. The developed SSM estimation model was as follows:

$$SSM = 0.539 + 0.044\sigma^0_{VV} + 0.444NDWI + 2.964NDWI^2 + 11.15NDWI^3 - 33.75NDWI^4 - 0.008\sigma^0_{VV} sec\theta + 0.016\sigma^0 NDWIsec\theta + 0.031\sigma^0_{VV} NDWI^2 sec\theta \quad (12)$$

Based on Sentinel-1 and Landsat 8 data, the soil water content of these sites were estimated by using Eq. (12). As seen in Fig. 3, the root mean square error of estimated SSM is 0.052 cm^3/cm^3, and the correlation coefficient between the estimated and measured soil volumetric moisture is 0.917. The correlation between the estimated and measured soil volumetric moisture was statistically significant at the 0.001 level.

4.2. SSM estimation model validation

In order to evaluate the accuracy of the semi-empirical model, a validation experiment was conducted for soil moisture estimation. Eq. (12) was employed to estimate SSM of another 51 validating sample data. The *in-situ* measured soil volumetric moisture was used as reference to calculate the root mean square error (RMSE) of the estimated SSM. As seen in Fig. 4, the RMSE is 0.053 cm^3/cm^3, and the correlation coefficient between the estimated and measured SSSM is 0.911. The correlation between the estimated and measured soil volumetric moisture was also statistically significant at the 0.001 level. The SSM estimation accuracy is similar with other republished researches based

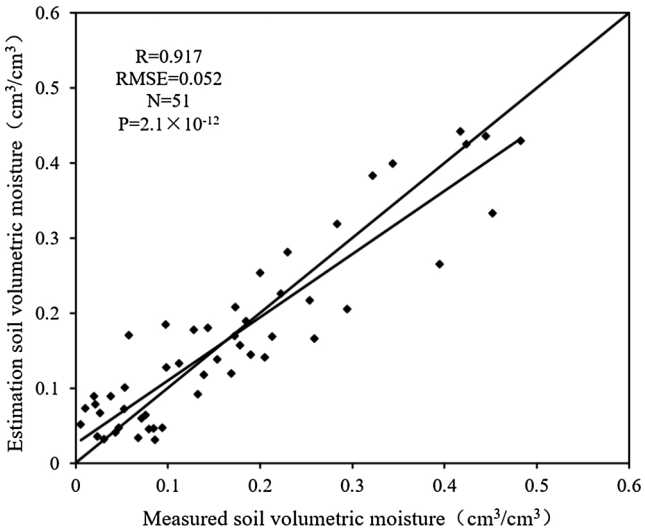

Fig. 3. Scatter plot between the measured and estimated soil volumetric moisture by the semi-empirical model based on the 51 training sample data. A 1:1 line is added in the plot.

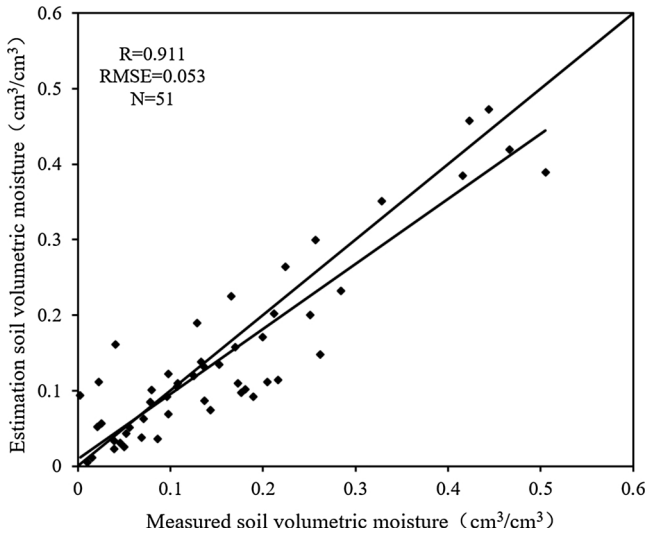

Fig. 4. Scatter plot between the measured and estimated soil volumetric moisture by the semi-empirical model based on the 51 validating sample data. A 1:1 line is added in the plot.

on Sentinel-1 data, of which the SSM RMSE is 0.059 cm^3/cm^3 (Gao et al., 2017). Compared to the republished research using a single satellite data (van der Schalie et al., 2017), the method by combing the Sentinel-1 and Landsat data acquired a higher accuracy.

To compare the difference between the semi-empirical model and empirical model, a linear empirical model between SSM and SAR data was also developed by a regression method based on the 51 sample data. The empirical model was also used to estimate the soil moisture of the 51 validation sample data. As seen in Fig. 5, the correlation coefficient between the estimated and measured SSM is 0.624, and the RMSE of the estimated SSM is 0.098 cm^3/cm^3. The correlation between the estimated and measured SSM was found as statistically significant at the 0.05 level.

As seen in Fig. 5, the estimated SSM by the empirical model was underestimated in the high soil moisture range, and overestimated in the low soil moisture range. However, the estimated SSM by the semi-empirical model was highly consistent with the measured value. Therefore, compared with the empirical model, the semi-empirical model reported a higher accuracy of SSM estimation.

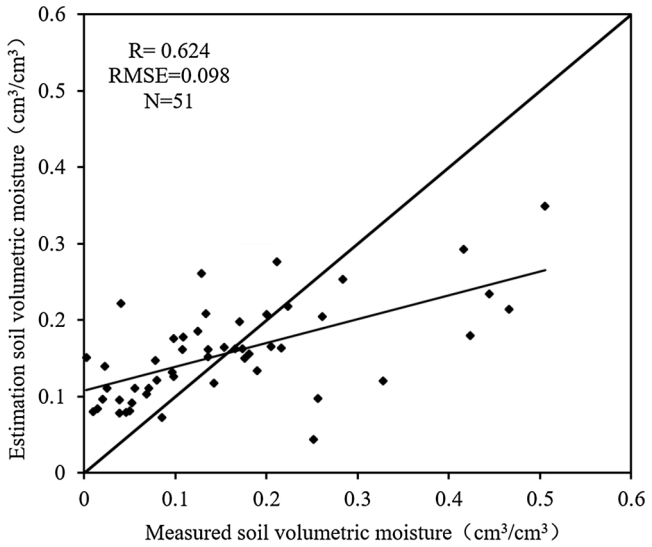

Fig. 5. Scatter plot between the measured and estimated soil volumetric moisture by the empirical model based on the 51 validating sample data. A 1:1 line is added in the plot.

4.3. The application of the semi-empirical SSM estimation model

The semi-empirical SSM estimation model was used to retrieve regional surface soil moisture from the Sentinel-1 SAR and Landsat 8 OLI data in the crop fields under clear-sky condition. Fig. 6 (a) and (b) are the surface soil moisture maps in UK on March 22, 2015 (a), and in Spain on January 20, 2015, respectively. As seen in Fig. 6(a), the soil moisture is plentiful around the 4 sites in UK. The estimated soil volumetric moisture of the 4 sites are distributed from 0.3 to 0.5 cm^3/cm^3, which are consistent with the *in-situ* measurement data (from 0.4 to 0.5 cm^3/cm^3). As seen in Fig. 6(b), the field is slightly droughty around the 20 sites in Spain. The estimated soil volumetric moisture is below 0.3 cm^3/cm^3. We also found similar results from the *in-situ* measurement data, which showed the soil moisture of 20 sites is from 0.1 to 0.3 cm^3/cm^3. Therefore, it can be concluded that the soil moisture estimated by the semi-empirical model was highly consistent with the measured value. The semi-empirical model proposed in this study is applicable for retrieving the SSM of the crop fields in a regional area.

5. Conclusions

The SSM estimation is more complex in a vegetation-covered region compared with bare soil region. Therefore, removing the influence of the vegetation layer on the radar backscattering coefficient, establishing reasonable vegetation scattering model and providing a model with reasonable precision are the keys for soil moisture remote sensing monitoring. In order to remove the effect of vegetation on SSM estimation, this paper first developed a vegetation water content model based on the normalized difference water index obtained from Landsat 8 OLI data. Then, by combining the water-cloud model and the new generation Sentinel-1 SAR data, a semi-empirical model was developed to estimate the soil water content over vegetated areas. The model achieved accurate soil moisture retrieval in the UK and Spain. The main conclusions of the present study are summarized as follows:

1) To effectively remove the effect of vegetation on the soil moisture estimation, NDVI, EVI and NDWI were compared in this study, and it was found that the NDWI built of the 1.57–1.65 μm band was the best for removing vegetation effect. The main reason is that SWIR1 channel was more sensitive to the vegetation water content.
2) Compared with the performances of the Sentinel-1 co-polarization VV and cross-polarization VH data in SSM estimation, the VV polarization obtain a higher SSM estimation accuracy. For the cross-polarized VH, the total backscattering contained much vegetation scattering information. Therefore, vegetation cover has a significant effect on SSM retrieval. However, the total backscattering at VV polarization has more soil backscattering information, and the vegetation effect is lower. So the Sentinel-1 VV polarization mode can obtain higher SSM estimation accuracy.
3) As the normalized difference water index obtained from Landsat 8 OLI data can be used to retrieve vegetation water content, we developed a modified water-cloud with NDWI. Based on the modified water-cloud model, a surface soil moisture estimation model was developed. The SSM estimation model obtained a high accuracy. The correlation coefficient between the estimated and measured soil volumetric moisture is 0.911, and the root mean square error of SSM was 0.053 cm^3/cm^3 Compared to the empirical model (R = 0.624, RMSE = 0.098), the semi-empirical model obtained a higher accuracy for soil moisture estimation. In addition, the estimated SSM from Sentinel-1 SAR has higher spatial resolution compared to other active microwave sensors, such as Soil Moisture and Ocean Salinit (SMOS) and SMAP.
4) A regional soil moisture mapping for crop fields can be realized at 20 m resolution and with 6-days interval using the developed SSM

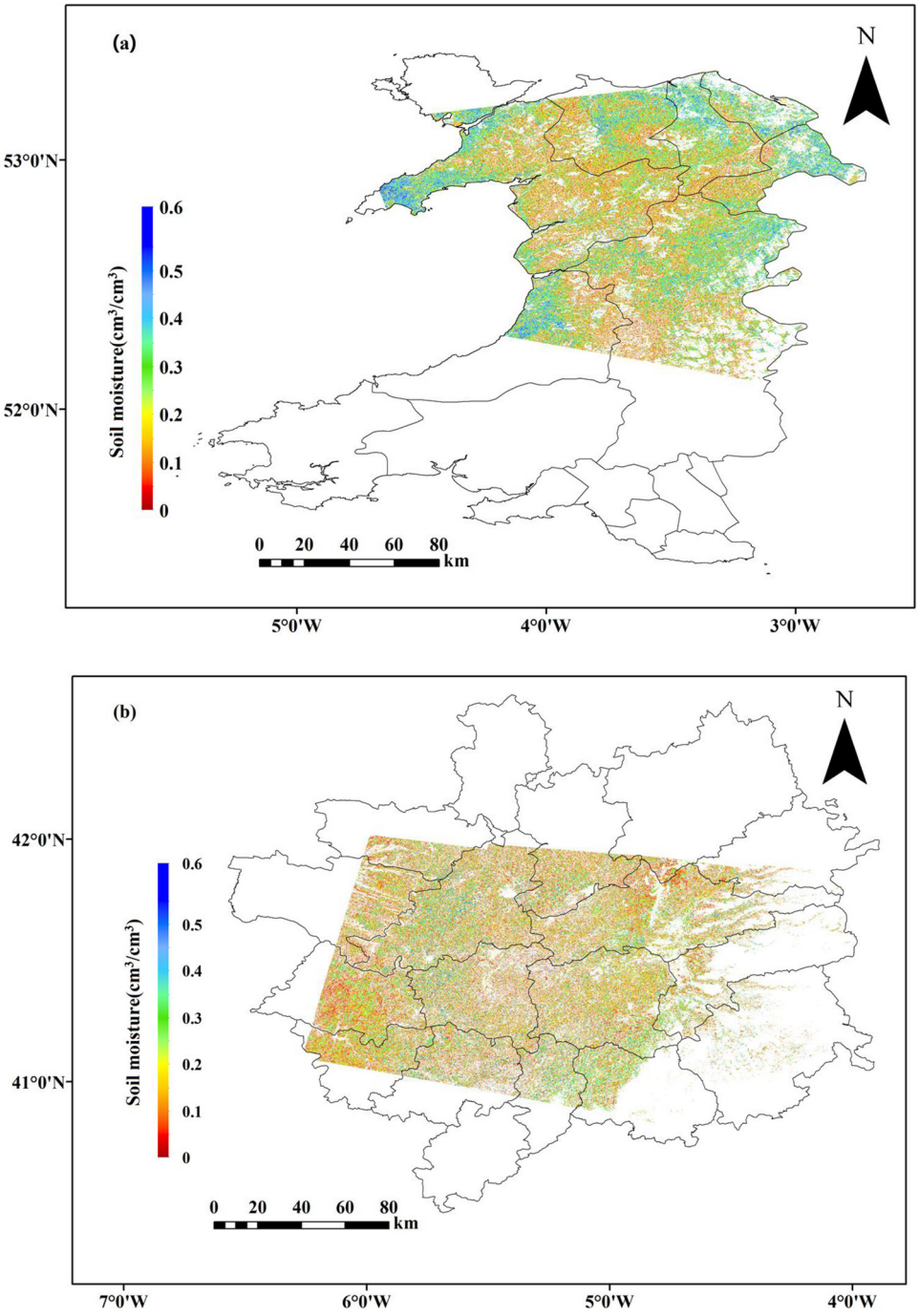

Fig. 6. Soil moisture mapping in UK in March 22, 2015(a); Soil moisture mapping in Spain in January 20, 2015(b).

estimation model based on Sentinel-1 SAR data. The SSM map can accurately indicate the draughty status in an area.

The SSM retrieval algorithm proposed in this study is simple and straightforward to implement, and the estimated SSM has very satisfactory accuracy at a high spatial and temporal resolution. However, the algorithm also has some limitations, which need to be addressed in the future. On one hand, there is still some error introduced due to ignoring the surface roughness and vegetation type. On the other hand, Landsat 8 data used herein have a low temporal resolution due to a long revisit cycle (16 days), so the high-frequency monitoring of an agricultural drought is limited. However, the latest launched Sentinel-2 satellite provides a revisit cycle of 5 days. The data could be downloaded after December 16 2015, and it has a spectral band near 1.61 μm which can be used to estimate the vegetation water content. Thus, in future work, the added value of Sentinel-2 providing high spatial and temporal resolution data with the Sentinel-1 SAR data can be explored to improve our ability to monitor agricultural drought and stress. In addition, surface roughness and the vegetation style need to be considered in building the model when this approach is expanded globally.

Acknowledgments

This research was supported by Projects of International Cooperation and Exchanges NSFC (NSFC-RCUK_STFC) (61661136005), the National Key Research and development Program of China (2016YFA0600703), “Six Talents Peak” high-level talent project in Jiangsu Province (2015-JY-013), and Projects of Key Laboratory of

Radiometric Calibration and Validation for Environmental Satellites , National Satellite Meteorological Center , China Meteorological Administration. Sincere thanks also go to all other participating colleagues and students for their dedications to these projects and the data collection campaigns. GPP's contribution has been supported by a UK Research Council award (STFC ST/N006836/1) and the FP7- People project ENViSIon-EO (project reference number 752094) and the author gratefully acknowledges the financial support provided by the aforementioned funding bodies.

References

Alexakis, D.D., Mexis, F.D.K., Vozinaki, A.E.K., Daliakopoulos, I.N., Tsanis, I.K., 2017. Soil moisture content estimation based on sentinel-1 and auxiliary earth observation products. A hydrological approach. Sensors (Switz.) 17, 1–16. http://dx.doi.org/10.3390/s17061455.

Anagnostopoulos, V., Petropoulos, G.P., Ireland, G., Carlson, T.N., 2017. A modernized version of a 1D soil vegetation atmosphere transfer model for improving its future use in land surface interactions studies. Environ. Model. Softw. 90, 147–156. http://dx.doi.org/10.1016/j.envsoft.2017.01.004.

Attema, E.P.W., Ulaby, F.T., 1978. Vegetation modeled as a water cloud. Radio Sci. 13, 357–364. http://dx.doi.org/10.1029/RS013i002p00357.

Baghdadi, N., Hajj, M., El, Zribi, M., Belin, E., 2016. Coupling sar C-band and optical data for soil moisture and leaf area index retrieval over irrigated grasslands irstea, UMR Tetis, 500 rue François Breton, 34093 Montp ellier cedex 5, France. IEEE J. Sel. Top. Appl. Earth Obs. Remote Sens. 9, 3551–3554. http://dx.doi.org/10.1109/JSTARS.2015.2464698.

Bai, X., He, B., Li, X., 2016. Optimum surface roughness to parameterize advanced integral equation model for soil moisture retrieval in prairie area using radarsat-2 data. IEEE Trans. Geosci. Remote Sens. 54, 2437–2449. http://dx.doi.org/10.1109/TGRS.2015.2501372.

Bao, Y., Zhang, Y., Wang, J., Min, J., 2014. Surface soil moisture estimation over dense crop using envisat ASAR and landsat TM imagery: an approach. Int. J. Remote Sens. 35, 6190–6212. http://dx.doi.org/10.1080/01431161.2014.951098.

Bolten, J.D., Crow, W.T., Jackson, T.J., Zhan, X., Reynolds, C.A., 2010. Evaluating the utility of remotely sensed soil moisture retrievals for operational agricultural drought monitoring. IEEE J. Sel. Top. Appl. Earth Obs. Remote Sens. 3, 57–66. http://dx.doi.org/10.1109/JSTARS.2009.2037163.

Ceccato, P., Gobron, N., Flasse, S., Pinty, B., Tarantola, S., 2002a. Designing a spectral index to estimate vegetation water content from remote sensing data : part 1 theoretical approach. Remote Sens. Environ. 82, 188–197. http://dx.doi.org/10.1016/S0034-4257(02)00037-8.

Ceccato, P., Gobron, N., Flasse, S., Pinty, B., Tarantola, S., 2002b. Designing a spectral index to estimate vegetation water content from remote sensing data: part 2. Validation and applications. Remote Sens. Environ. 82, 198–207. http://dx.doi.org/10.1016/S0034-4257(02)00036-6.

Chauhan, S., Srivastava, H.S., 2016. Comparative Evaluation of the Sensitivity of Multi-Polarised Sar and Optical Data for Various Land Cover 4. pp. 1–14.

Chen, D., Huang, J., Jackson, T.J., 2005. Vegetation water content estimation for corn and soybeans using spectral indices derived from MODIS near- and short-wave infrared bands. Remote Sens. Environ. 98, 225–236. http://dx.doi.org/10.1016/j.rse.2005.07.008.

Cheng, X., Yang, G., Xu, X., Chen, T., Wang, D., 2014. Inferred Water content of winter wheat based on Ground hyperspectral and remote sensing data of TM5. J. Triticeae Crop. 34, 227–233.

Chuvieco, E., Riaño, D., Aguado, I., Cocero, D., 2002. Estimation of fuel moisture content from multitemporal analysis of landsat thematic mapper reflectance data: applications in fire danger assessment. Int. J. Remote Sens. 23, 2145–2162. http://dx.doi.org/10.1080/01431160110069818.

Dorigo, W.A., Wagner, W., Hohensinn, R., Hahn, S., Paulik, C., Xaver, A., Gruber, A., Drusch, M., Mecklenburg, S., Van Oevelen, P., Robock, A., Jackson, T., 2011. The International soil moisture network: a data hosting facility for global in situ soil moisture measurements. Hydrol. Earth Syst. Sci. 15, 1675–1698. http://dx.doi.org/10.5194/hess-15-1675-2011.

ELVIDGE, C.D., LYON, R.J.P., 1985. Estimation of the vegetation contribution to the 1·65/2·22μm ratio in airborne thematic-mapper imagery of the Virginia range. Nev. Int. J. Remote Sens. 6, 75–88. http://dx.doi.org/10.1080/01431168508948425.

Gao, B.C., 1996. NDWI - a normalized difference water index for remote sensing of vegetation liquid water from space. Remote Sens. Environ. 58, 257–266. http://dx.doi.org/10.1016/S0034-4257(96)00067-3.

Gao, Q., Zribi, M., Escorihuela, M.J., Baghdadi, N., 2017. Synergetic use of sentinel-1 and sentinel-2 data for soil moisture mapping at 100m resolution. Sensors (Switz.) 17. http://dx.doi.org/10.3390/s17091966.

González-Zamora, Á., Sánchez, N., Martínez-Fernández, J., Gumuzzio, Á., Piles, M., Olmedo, E., 2015. Long-term SMOS soil moisture products: a comprehensive evaluation across scales and methods in the Duero Basin (Spain). Phys. Chem. Earth 83–84, 123–136. http://dx.doi.org/10.1016/j.pce.2015.05.009.

He, L., Qin, Q., Ren, H., Du, J., Meng, J., Du, C., 2016. Soil moisture retrieval using multitemporal Sentinel-1SAR data in agricultural areas. Trans. Chin. Soc. Agric. Eng. 32, 142–148.

Hégarat-mascle, S.Le, Zribi, M., Alem, F., Weisse, A., Loumagne, C., 2002. Soil moisture estimation from ERS / SAR Data: toward an operational methodology. IEEE Xplore 40, 2647–2658.

Huang, J., Chen, D., Cosh, M.H., 2009. Sub-pixel reflectance unmixing in estimating vegetation water content and dry biomass of corn and soybeans cropland using normalized difference water index (NDWI) from satellites. Int. J. Remote Sens. 30, 2075–2104. http://dx.doi.org/10.1080/01431160802549245.

Huete, A., Justice, C., Liu, H., 1994. Development of vegetation and soil indices for MODIS-EOS. Remote Sens. Environ. 49, 224–234. http://dx.doi.org/10.1016/0034-4257(94)90018-3.

Jackson, T.J., Chen, D., Cosh, M., Li, F., Anderson, M., Walthall, C., Doriaswamy, P., Hunt, E.R., 2004. Vegetation water content mapping using landsat data derived normalized difference water index for corn and soybeans. Remote Sens. Environ. 92, 475–482. http://dx.doi.org/10.1016/j.rse.2003.10.021.

Jiang, J., Hu, D., Li, Y., Tang, X., Li, J., 2015. Research of soil moisture retrieval model of wheat covered surface based on MIMICS model. J. Triticeae Crop. 35, 707–713.

Kumar, K., Suryanarayana Rao, H.P., Arora, M.K., 2015. Study of water cloud model vegetation descriptors in estimating soil moisture in solani catchment. Hydrol. Process. 29, 2137–2148. http://dx.doi.org/10.1002/hyp.10344.

Lee, J.S., Jurkevich, L., Dewaele, P., Wambacq, P., Oosterlinck, A., 1994. Speckle filtering of synthetic aperture radar images: a review. Remote Sens. Rev. 8, 313–340. http://dx.doi.org/10.1080/02757259409532206.

Leroux, D.J., Kerr, Y.H., Bitar, A.Al, Bindlish, R., Jackson, T.J., Berthelot, B., Portet, G., 2007. Comparison between SMOS, VUA, ASCAT, and ECMWF soil moisture products Over Four watersheds in U.S. IEEE Trans. Geosci. Remote Sens. 54, 1–13.

Lu, L., Luo, G.-P., Wang, J.-Y., 2014. Development of an ATI-NDVI method for estimation of soil moisture from MODIS data. Int. J. Remote Sens. 35, 3797–3815. http://dx.doi.org/10.1080/01431161.2014.919677.

Maggioni, V., Panciera, R., Walker, J.P., Rinaldi, M., Paruscio, V., Kalma, J.D., Kim, E.J., 2006. A multi-sensor approach for High Resolution airborne soil moisture mapping. 30th Hydrol. Water Resour. Symp. 4.

Mao, K.B., Tang, H.J., Zhang, L.X., Li, M.C., Guo, Y., Zhao, D.Z., 2008. A method for retrieving soil moisture in Tibet region by utilizing microwave index from TRMM/TMI data. Int. J. Remote Sens. 29, 2903–2923. http://dx.doi.org/10.1080/01431160701442104.

Mattia, F., Satalino, G., Dente, L., Pasquariello, G., 2006. Using a priori information to improve soil moisture retrieval from ENVISAT ASAR AP data in semiarid regions. IEEE Trans. Geosci. Remote Sens. 44, 900–911. http://dx.doi.org/10.1109/TGRS.2005.863483.

Pablos, M., Martínez-Fernández, J., Sánchez, N., González-Zamora, Á., 2017. Temporal and spatial comparison of agricultural drought indices from moderate resolution satellite soil moisture data over northwest Spain. Remote Sens. 9. http://dx.doi.org/10.3390/rs9111168.

Paloscia, S., Pettinato, S., Santi, E., Notarnicola, C., Pasolli, L., Reppucci, A., 2013. Soil moisture mapping using Sentinel-1 images: algorithm and preliminary validation. Remote Sens. Environ. 134, 234–248. http://dx.doi.org/10.1016/j.rse.2013.02.027.

Patel, P., Srivastava, H.S., Panigrahy, S., Parihar, J.S., 2006. Comparative evaluation of the sensitivity of multi-polarized multi-frequency SAR backscatter to plant density. Int. J. Remote Sens. 27, 293–305. http://dx.doi.org/10.1080/01431160500214050.

Petropoulos, G.P., McCalmont, J.P., 2017. An operational in situ soil moisture & soil temperature monitoring network for West Wales, UK: the WSMN network. Sensors (Switz.) 17. http://dx.doi.org/10.3390/s17071481.

Petropoulos, G.P., Ireland, G., Srivastava, P.K., Ioannou-Katidis, P., 2014. An appraisal of the accuracy of operational soil moisture estimates from SMOS MIRAS using validated in situ observations acquired in a Mediterranean environment. Int. J. Remote Sens. 35, 5239–5250. http://dx.doi.org/10.1080/2150704X.2014.933277.

Petropoulos, G.P., Srivastava, P.K., Piles, M., Pearson, S., 2018. Earth observation-based operational estimation of soil moisture and evapotranspiration for agricultural crops in support of sustainable water management. Sustainability 10 181.

Pierdicca, N., Pulvirenti, L., Bignami, C., Ticconi, F., 2013. Monitoring soil moisture in an agricultural test site using SAR data: design and test of a pre-operational procedure. IEEE J. Sel. Top. Appl. Earth Obs. Remote Sens. 6, 1199–1210. http://dx.doi.org/10.1109/JSTARS.2012.2237162.

Piles, M., Petropoulos, G.P., Sánchez, N., González-Zamora, Á., Ireland, G., 2016. Towards improved spatio-temporal resolution soil moisture retrievals from the synergy of SMOS and MSG SEVIRI spaceborne observations. Remote Sens. Environ. 180, 403–417. http://dx.doi.org/10.1016/j.rse.2016.02.048.

Prakash, R., Singh, D., Pathak, N.P., 2012. A fusion approach to retrieve soil moisture with SAR and optical data. IEEE J. Sel. Top. Appl. Earth Obs. Remote Sens. 5, 196–206. http://dx.doi.org/10.1109/JSTARS.2011.2169236.

Rouse, J.W., Haas, R.H., Schell, J.A., Deering, D.W., 1973. Monitoring vegetation systems in the Great Okains with ERTS. Third Earth Resour. Technol. Satell. Symp. 1, 325–333.

Santamaria-Artigas, A., Mattar, C., Wigneron, J.P., 2016. Application of a combined optical-passive microwave method to retrieve soil moisture at regional scale over Chile. IEEE J. Sel. Top. Appl. Earth Obs. Remote Sens. 9, 1493–1504. http://dx.doi.org/10.1109/JSTARS.2015.2512926.

Seneviratne, S.I., Corti, T., Davin, E.L., Hirschi, M., Jaeger, E.B., Lehner, I., Orlowsky, B., Teuling, A.J., 2010. Investigating soil moisture-climate interactions in a changing climate: a review. Earth-Sci. Rev. http://dx.doi.org/10.1016/j.earscirev.2010.02.004.

Tian, G., 1991. Methods for monitoring soil moisture using remote sensing technique. J. Remote Sens. 6, 89–98.

Torres-Rua, A.F., Ticlavilca, A.M., Bachour, R., McKee, M., 2016. Estimation of surface soil moisture in irrigated lands by assimilation of landsat vegetation indices, surface energy balance products, and relevance vector machines. Water (Switz.) 8. http://dx.doi.org/10.3390/w8040167.

van der Schalie, R., de Jeu, R.A.M., Kerr, Y.H., Wigneron, J.P., Rodríguez-Fernández, N.J.,

Al-Yaari, A., Parinussa, R.M., Mecklenburg, S., Drusch, M., 2017. The merging of radiative transfer based surface soil moisture data from SMOS and AMSR-E. Remote Sens. Environ. 189, 180–193. http://dx.doi.org/10.1016/j.rse.2016.11.026.

Verstraeten, W.W., Veroustraete, F., Van Der Sande, C.J., Grootaers, I., Feyen, J., 2006. Soil moisture retrieval using thermal inertia, determined with visible and thermal spaceborne data, validated for European forests. Remote Sens. Environ. 101, 299–314. http://dx.doi.org/10.1016/j.rse.2005.12.016.

Wang, J., Ding, J.L., Chen, W.Q., Yang, A.X., 2017. Microwave modeling of soil moisture in Oasis regional scale based on Sentinel-1 radar images. J. Infrared Millim. Waves 36, 120–127.

Whyte, A., Fredinos, K., Petropoulos, G.P., 2018. A New Synergistic Approach for Monitoring Wetlands Using Sentinels -1 and 2 data With Object-based Machine Learning Algorithms. Environ. Modell. Softw. 104, 40–57.

Yi, Y., Yang, D., Chen, D., Huang, J., 2007. Retrieving crop physiological parameters and assessing water deficiency using MODIS data during the winter wheat growing period. Can. J. Remote Sens. 33, 189–202. http://dx.doi.org/10.5589/m07-025.

Zeng, X., Xing, Y., Shan, W., Zhang, Y., Wang, C., 2017. Soil water content retrieval based on Sentinel-1A and landsat 8 image for Bei'an-Heihe expressway. Chin. J. Eco-Agric. 25, 118–126.

Zhang, J., Xu, Y., Yao, F., Wang, P., Guo, W., Li, L., Yang, L., 2010. Advances in estimation methods of vegetation water content based on optical remote sensing techniques. Sci. China Technol. Sci. 53, 1159–1167. http://dx.doi.org/10.1007/s11431-010-0131-3.

Zhang, D., Zhou, G., 2016. Estimation of soil moisture from optical and thermal remote sensing: a review. Sensors 16, 1308. http://dx.doi.org/10.3390/s16081308.

Zheng, X., Ding, Y., Zhao, K., Jiang, T., Li, X., Zhang, S., Li, Y., Wu, L., Sun, J., Ren, J., Zhang, X., 2014. Estimation of vegetation water content from landsat 8 OLI data. Spectrosc. Spectr. Anal. 34, 3385–3390.

Zribi, M., Dechambre, M., 2003. A new empirical model to retrieve soil moisture and roughness from C-band radar data. Remote Sens. Environ. 84, 42–52. http://dx.doi.org/10.1016/S0034-4257(02)00069-X.